Collision-Induced Desorption and Reaction on Hydrogen-Covered Al(111) Single Crystals: Hydrogen *in* Aluminum?

Elizabeth L. Crane and Ralph G. Nuzzo*

School of Chemical Sciences and the Frederick Seitz Materials Research Laboratory, University of Illinois at Urbana-Champaign, Urbana, Illinois 61801

Received: October 19, 2000; In Final Form: February 1, 2001

We examine the recombination and desorption of hydrogen from an aluminum(111) surface focusing on desorption processes that lead to the formation of dihydrogen and aluminum hydride (presumably alane). In addition to simple temperature-programmed reaction spectroscopy (TPRS), we examine the perturbations which occur to the desorption kinetics of these species as a result of the energy transfer due to collisions of a xenon beam at 1.6, 2.8, and 3.6 eV with a hydrogen covered surface. Whereas the recombinative desorption of dihydrogen from an Al(111) surface nominally follows an unusual zero-order rate law, bombardment of a hydrogen-covered surface with an energetic xenon atom leads to a kinetic profile more closely modeled by a higher reaction order. It also was found that upon exposure to the beam, the peak area (and thus the desorption yield) for the H_2 desorption was reduced 5−25% depending on the length of exposure whereas for the aluminum hydride the percent reduction ranged from 10−80%. This suggests that both a stimulated etching and a change in state result from the beam exposure. We present evidence that suggests that the initial state of the bound hydrogen may involve at least in part a subsurface occupation.

Introduction

Aluminum thin films, especially those obtained via chemical vapor (CVD) or plasma-enhanced sputtering depositions have several properties that make them particularly attractive materials for use in advanced electronics fabrication.[1−14] Among these are the low resistivity and high stability of the metal and low deposition temperatures.[2,15] Consequently, the surface chemistries of aluminum have been the focal point of much research. In order to fully understand the complex mechanisms of aluminum CVD, it is imperative that the elementary surface reaction mechanisms involving adsorbates bound to the surface of this metal be understood with the hope that these insights might help improve their efficiencies more generally.[16−18] Additionally, the study of the interactions of hydrogen with metals is an area which has been afforded a great deal of attention due to its importance in understanding embrittlement.[19−23] At least in part for these reasons, considerable effort has been put into studying the seemingly simple reactions of hydrogen with an aluminum single crystal surface.[24−35] These studies have shown that this adsorbate system demonstrates remarkable properties, especially as regards the kinetics of hydrogen atom recombination on low-index single crystal surfaces.

As a general rule, the recombination of atomic hydrogen and the subsequent desorption of H_2 from a metal surface are strongly linked to the dynamics of the adsorbate diffusion on the surface and the elementary reaction rates for recombination. Several limiting behaviors are possible. The most simple kinetic case arises when the reaction velocity is limited by the elementary reaction rate for recombination for a H atom overlayer freely diffusing as a 2-D lattice gas. Such systems exhibit a second-order rate law for H_2 desorption (i.e., one which varies as the square of the hydrogen coverage, q_H). Representative examples of materials exhibiting this type of limiting rate behavior include Si(111),[26, 27] Pd(110),[17] Cu(110),[37,38] Be(0001),[19] and Pt(100).[39]

A more complex case arises when the global rate becomes limited by the diffusion velocity. In this instance, a first-order rate law is expected. Such behavior has been reported for hydrogen desorption from a Pt(110)(1x2) surface.[40] It is also possible to obtain a first-order rate law when the H-diffusion process is constrained. For example, pinning H atoms at lattice sites (and thus allowing only one partner to freely diffuse) can yield an apparent first-order rate law for H_2 desorption.[36]

The desorption of H_2 from aluminum demonstrates what is perhaps one of the more unusual rate behaviors described in the literature. When atomic hydrogen (used because molecular hydrogen does not spontaneously dissociate on the aluminum surface) is deposited on a clean aluminum single crystal, its subsequent thermal desorption follows a power rate law which is closely (and best) modeled by zero-order kinetics.[26,29,30,41] Perhaps more interesting, though, is the finding that this desorption competes kinetically with a metal etching pathway that leads to the concurrent desorption of aluminum hydride species.[26,30] This latter product partitioning varies sensitively with the structure of the surface, being especially favored on Al(111),[24,42] as well as with the heating rate used to initiate the desorption events.[42]

A general agreement has not been reached for the reasons underlying this behavior, one that is so unlike that of other metals. Nozoye et al. argued that the aluminum hydride product (presumably alane) is the primary desorbant with the dihydrogen being an ionization-derived fragment of this compound.[30] Alternately, Winkler and his co-workers modeled the system as an array of $p(1\times1)$ islands[27,42] (as did Paul for an Al(100) surface[28]). Winkler suggested that the equilibrium condition which exists between the islands and a two-dimensional (2D) lattice gas gives rise to the zero-order desorption kinetics

10.1021/jp003862v CCC: $20.00 © 2001 American Chemical Society
Published on Web 03/27/2001

observed for the hydrogen and produces a half order desorption profile for the aluminum hyride species.

The current study verifies and extends aspects of these earlier experimental findings. We further add several new insights gained by examining the desorption kinetics of the system following its exposure to a hyperthermal, inert-atom beam. The results, when taken together, point to a potential change in kinetic order (from zero to either first or second) after such an exposure, a perturbation that we believe mirrors changes in the hydrogen bonding states on the surface. Taken together with a wealth of data available in the literature on hydrogen embrittlement,[19−23] we believe a model of the H+Al(111) system involving both surface and subsurface occupancies must be considered.

Experimental Section

The experiments for this study were performed in a three-stage UHV chamber that has been described in detail previously.[43,44] The first two stages of the chamber are used for beam generation. The beam is formed by a constant adiabatic expansion of the gas from a 25 mm molybdenum aperture. The beam source can be resistively heated from room temperature to ∼850 K enabling a wide range of incident beam energies. This entire assembly is mounted on an $X-Y-Z$ translational manipulator to allow precise alignment of the beam axis. A 10-in. diffusion pump maintained the low pressure within this first stage. A 400 mm diameter nickel skimmer mounted on the inside wall of this first stage was used to form the beam. The distance between the skimmer and nozzle was approximately 1 cm and could be adjusted to optimize the beam intensity and velocity distribution.

The next stage serves to further collimate the expanding beam. This stage is separated from the scattering/analysis chamber (described below) with a manual gate valve and pumped with a liquid nitrogen-trapped 10-inch diffusion pump.

The gas mixture used in these experiments was 1% Xe in 99.99995% pure He (Matheson). The signal for the most common isotope of the Xe ($m/e = 131$) was calibrated against a fixed background pressure giving an absolute flux of the order of $2(+1) \times 10^{13}$ atom/cm^2/s.

The third stage is the UHV chamber used for analysis and has a base pressure $<2 \times 10^{-10}$ Torr. It is pumped with a liquid nitrogen-trapped 10-in. diffusion pump (5000 L/s). The chamber is equipped with two quadrupole mass spectrometers, each shrouded and differentially pumped by 30 L/s ion pumps. A single pass cylindrical mirror analyzer with conical electron gun (PHI) was used to examine the surface composition by Auger electron spectroscopy (AES). An ion gun was used for sputtering the substrate with Ar^+.

The experiments utilized several different 8mm Al(111) crystals mounted to button heaters with tantalum support wires passed through notches cut in the sides of the substrate. The temperature was controlled with a Eurotherm temperature controller and monitored with a chromel-alumel thermocouple lodged in a hole spark-cut in the side of the sample. The crystals could be cooled and heated through a range of 90 to 750 K. The cleaning protocol used, which has been described elsewhere, involved sputtering the crystal with 1 keV Ar^+ ions at 650 K, followed by annealing at 750 K for 5 min. The surfaces were checked by AES to ascertain their cleanliness. The heating rate used for the TPRS measurements was 4 K/s.

Exposures to hydrogen (ultra high purity, MG Industries) were made through a precision leak valve. The molecular hydrogen was dissociated using a hot tungsten filament (0.25 mm diameter resistively heated at 6 A) held approximately 2 cm from the crystal face. Exposures are recorded in langmuirs (1 langmuir $= 10^{-6}$ Torr s). The pressures cited here, monitored with a UHV ionization gauge, are not corrected for sensitivity nor for the dissociation efficiency of the tungsten filament and therefore the reported adsorbate exposures are only approximate.

Results

We shall present the results of these experiments in two parts. In the first we describe the results obtained from a standard temperature-programmed reaction spectroscopy (TPRS) study. These results provide a benchmark against which to compare the different behaviors seen in the other parts of the study. The second section examines the effects on both the surface and the desorption kinetics which result from the impingement of an energetic beam of Xe on the hydrogen-covered surface.

Figure 1 shows the TPRS traces for hydrogen ($m/e = 2$, Figure 1a) and a mass representative of aluminum hydride species ($m/e = 29$, Figure 1b). The latter are most likely reflective of either an alane (AlH_3) monomer or dimer. Clean aluminum surfaces do not dissociate H_2. In order to deposit H atoms a clean Al(111) surface was exposed to 5×10^{-7} Torr of hydrogen while the surface was held ∼2 cm from a tungsten filament through which a 6A current was passed. For the data shown in this figure, the sample was grounded during the exposure (charging results from emission from the tungsten filament if the latter is neglected, see Supporting Information). The spectra obtained show lineshapes similar to those reported in previous studies.[26,27,41,42] Notably, we see a common leading edge with the peak temperature increasing with increasing surface coverage (inset of Figure 1a); the trailing edge falls quickly in each case, generating a highly asymmetric lineshape. These quantitative aspects of the data tend to suggest that the desorption of H_2 occurs via a zero-order kinetic process (i.e., the initial rate is not governed by the surface coverage of H) rather than the second-order behavior expected for a recombination process. Figure 1b follows the desorption of aluminum hydride fragments. The signal to background level for the latter data are lower but it appears that, again, a common leading edge and increasing peak maximum temperature reflective of zero-order kinetics are seen. The desorption of AlH_x species has been reported by other researchers although its presence[41] and reaction order[45] are not universally agreed upon. In addition to the $m/e = 29$ profile, other aluminum hydride fragments were followed and displayed similar characteristics ($m/e = 27$, 28, and 30). The $m/e = 30$ peak suggests that at least some (or perhaps all) of the Al-H species seen originate from the desorption of alane (AlH_3). We are not certain if oligomers of alane (e.g., Al_2H_6) are also present in the product flux (although Nozoye et al. have reported their presence[30]).

Some aspects of the data suggest that the H_2 desorption trace does not directly follow that of the alane species. We observed, for example, that the highest peak temperature for the dihydrogen desorption was ∼340 K for the highest exposures exceeding saturation (300 L) but only ∼330 K for the aluminum hydride. This result (in agreement with the results of other studies[24,27,29,30]) indicates that these traces monitor, at least in part, two distinct desorbing species. The data clearly establish that the phase-behaviors of the H atoms on the Al(111) surface are exceedingly complex; in some regards they appear to follow more from the properties expected for the decomposition of a solid hydride phase than from the recombination dynamics of H atoms bound on a 2D surface lattice. The thermal activation of the desorption processes thus deviates significantly from the behaviors expected for a simple H on metal system.

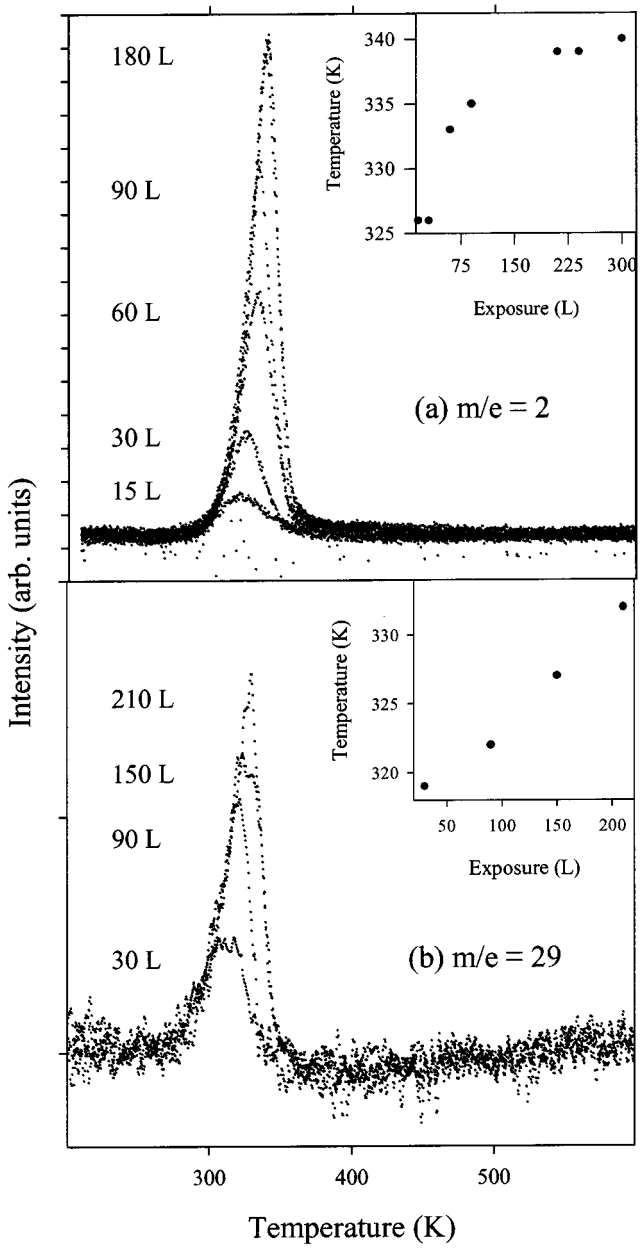

Figure 1. TPR spectra of the major components of desorption from a hydrogen covered aluminum surface: (a) $m/e = 2$ (H_2^+) and (b) $m/e = 29$ (AlH_2^+) at different degrees of coverage as indicated in the figure (1 L = 1×10^{-6} Torr sec.). The inset in each shows the temperature of the peak maximum in relation to the exposure.

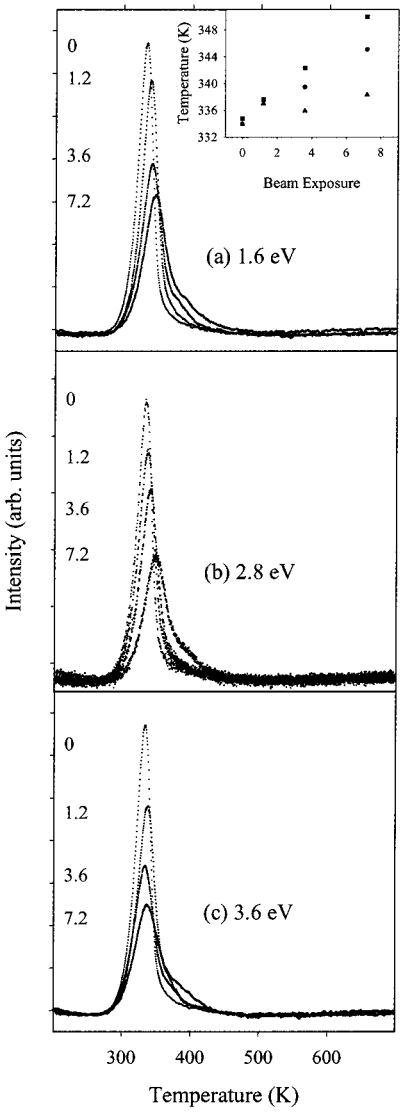

Figure 2. TPR spectra of the $m/e = 2$ (H_2^+) species after exposure of a hydrogen covered surface to the xenon beam for the fluxes indicated in the figure (the integrated flux as measured in units of 10^{16} collisions/cm^2). Three beam energies were used: (a) 1.6 eV, (b) 2.8 eV, and (c) 3.6 eV. The inset in the low energy beam plot depicts the temperature of the maximum desorption in relation to the exposure to the beam for ●= 1.6 eV, ■= 2.8 eV, and ▲ = 3.6 eV.

Hyperthermal atom scattering, the focal point of the studies presented here, provides a complementary way to explore the energetics and dynamics of surface adsorbate systems. We therefore examined the effect of the energy transfer due to the energetic inert gas atom beam (Xe) on the hydrogen-covered surface. Figure 2 shows the evolution of the TPR spectra as the hydrogen-covered surfaces are exposed to the beam for increasing lengths of time, ranging for these data from 10 minutes to 1 h. Three representative energies, 1.6, 2.8, and 3.6 eV, were used to characterize the effect of the impinging atoms on the surface (Figure 2a−c, respectively). We observe that the common leading edge, increasing peak maximum, and steep trailing edge associated with the previous traces become much less pronounced. Now as the amount of hydrogen on the surface decreases (resulting from a longer exposure of an initially saturated surface to the beam), the temperatures for the peak maxima increase (i.e., lower surface coverages of H lead to increasing temperatures for the maximum rate of desorption). The latter trend is normally indicative of a second-order desorption profile and in its simplest form implies that the process is dependent on the rate of the recombination of mobile surface atoms. This feature will be addressed in the following section.

As one would predict, it is the highest energy beam (3.6 eV, Figure 2c) that produces the most dramatic reduction in surface coverage due to beam induced desorption. The peak desorption temperatures associated with these spectra are similar to those found for the lower energy cases. For example, the 3.6 eV beam yields a peak maximum for H_2 desorption at 346 K after an exposure of 7.2×10^{16} collisions/cm^2, while a 1.6 eV energy shows a peak maximum desorption temperature of 350 K for the same total flux. The data, while showing modest quantitative differences (see below), are suggestive of an energy scaling in a stimulated desorption process.

The characteristics of the collision-induced desorption process (CID) are clearly seen by considering the data obtained for the

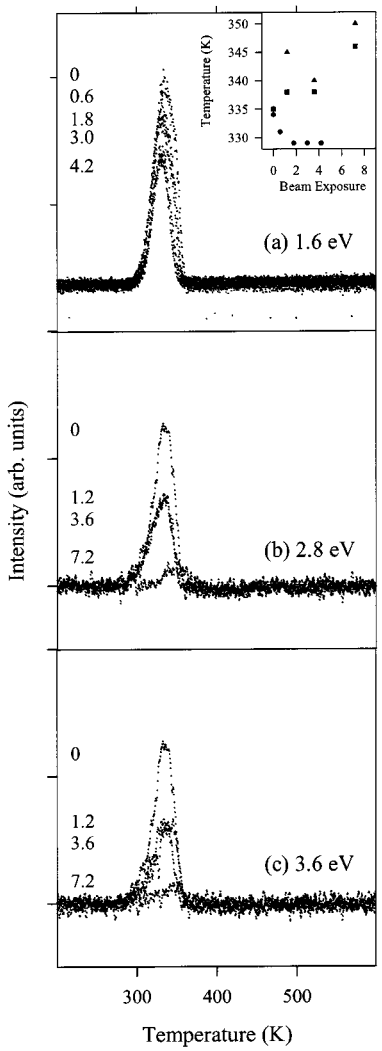

Figure 3. TPR spectra of the $m/e = 30$ (AlH_3^+) species after exposure of a hydrogen covered surface to the xenon beam for the fluxes indicated in the figure (the integrated flux as measured in units of 10^{16} collisions/cm^2). Three beam energies were used: (a) 1.6 eV, (b) 2.8 eV, and (c) 3.6 eV. The inset in the low energy beam plot depicts the temperature of the maximum desorption in relation to beam exposure for ●= 1.6 eV, ■= 2.8 eV, and ▲= 3.6 eV.

alane species. Figure 3 shows TPR spectra for the aluminum hydride fragment ($m/e = 30$, in this case) after exposure to the xenon beam. The yield of the aluminum hydride is markedly reduced with the beam exposure; lesser shifts are seen in the peak desorption temperatures however. The 2.8 or 3.6 eV beams are seen to completely deplete the alane forming state; in each case, a 7.2×10^{16} collisions/cm^2 exposure is sufficient to largely remove this species from the products formed even though significant quantities of H remain bound to the surface. This may indicate that the bound state(s) of the hydrogen which leads to the desorption of the molecular hydrogen does not produce aluminum hydride species simultaneously.

In the TPRS traces for the alane species seen in Figure 3, we notice that the sharp trailing edge and common leading edge are largely preserved. The marked broadening and shifting observed in the dihydrogen desorption is not as evident in this case, perhaps in part because of the significant loss of peak height due to a collision-induced desorption.

Auger spectra were taken after the beam exposures and these showed a slight increase in impurities on the aluminum surface but with no significant correlation with the length of the exposure. Auger spectra taken after 1.2×10^{16} and 7.2×10^{16} collisions/cm^2 beam exposures, for example (available as supplemental materials), show similar carbon and oxygen contamination. These increases (on the order of a few atomic percent) are consistent with the amount of impurities that we find deposit as a result of the outgassing of the AES spectrometer. Thus, the marked differences seen between the highest and lowest Xe fluxes are not a result of surface contamination impeding the desorption process.

Discussion

There are several factors that distinguish aluminum from other metals and therefore cause the reactions of hydrogen on it to differ in marked ways. We shall highlight a few of the properties that we believe may lead to the unique thermal behaviors of hydrogen bound to an Al(111) single crystal surface.

The primary factor that prohibits the dissociative adsorption of molecular hydrogen on aluminum is lack of energetically accessible d-orbitals.[46] Generally, for dissociative chemisorption to take place there must be favorable symmetry between the H_2 molecule and the surface and a filling of d-holes. Where d-orbitals are energetically accessible (e.g., as in most of the transition metals), dissociative chemisorption occurs with no apparent activation energy. Unlike the latter metals, aluminum does not have partially filled d-orbitals. This raises the energy for dissociating hydrogen on the surface to energies greater than 1 eV.[46] It is also of importance that the resultant energy minimum for H bound at the surface lies close to or perhaps several kcals/mol above the zero energy level for dihydrogen and aluminum.[19] This behavior is reminiscent of the properties of metals such as beryllium and copper, which are reported to have activation energies close to 0.7 eV and adsorption minima close to the Al+H_2 zero energy level.[19]

It is important to note that barriers to the dissociation of H_2 are not an uncommon feature of M+H_2 energy surfaces. The dissociative adsorption of hydrogen on both nickel and palladium, metals which efficiently dissociate H_2 even at very low temperatures,[47,48] is also an activated process.[19] For these cases, however, the maxima of the energy surfaces for the conversion of the precursor to the chemisorbed form lie below the zero energy level.[19]

As noted above, the recombination and desorption of hydrogen from metal surfaces (e.g., palladium[49] and copper[50]) typically follow a rate law governed by a second-order dependence on the surface coverage of hydrogen. In a TPRS experiment, this manifests itself as peak maxima that shift downward in temperature as the surface coverage increases. Such line shapes are not seen for the hydrogen on aluminum system and we now consider several models which might rationalize the broader range of behaviors illustrated by the data obtained from the hyperthermal scattering studies. Before doing so, however, it is useful to examine the quantitative aspects of the energetic barriers for the various desorption processes and analyze in greater depth both the dynamics and larger effects of the xenon beam on the product partitioning seen.

We shall first consider the activation energy for desorption in those cases where the atom beam was not utilized. For the reasons developed earlier, we model the process on the basis of a simple zero-order rate law for the desorption of H_2. The leading edge of the hydrogen desorption intensity in Figure 1 was fit using an Arrhenius equation relationship by plotting the log of the intensity against $1/T$. The fit is quite good and the slope of the resultant straight line gave an activation energy for desorption[51] of 0.74 eV, a value which is in good agreement with those previously reported in the literature.[27,29] A similar

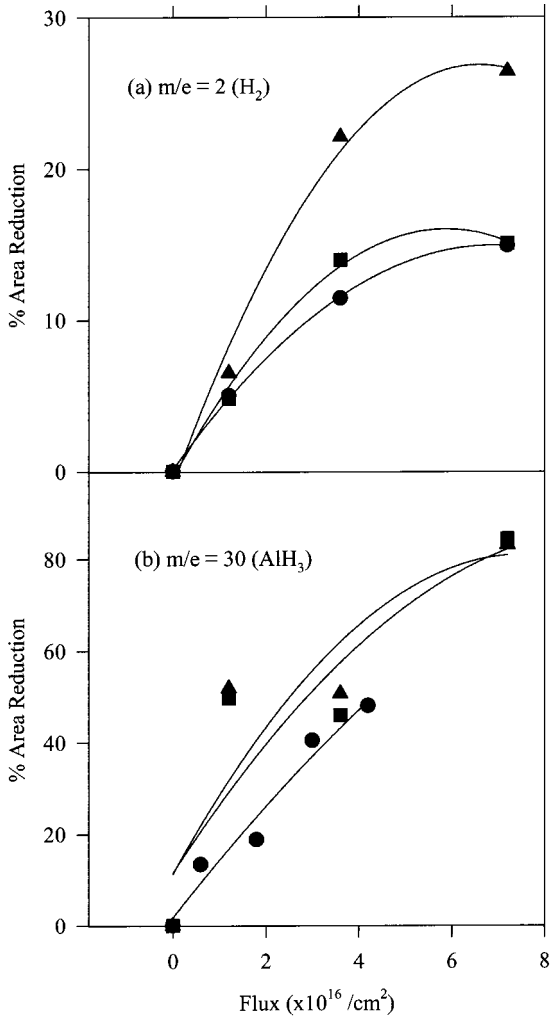

Figure 4. The percent reduction in peak area after exposure of a hydrogen covered surface to xenon beams of various energies (● = 1.6 eV, ■ = 2.8 eV, and ▲ = 3.6 eV) for (a) $m/e = 2$ (H_2^+) and (b) $m/e = 30$ (AlH_3^+). The lines are to guide the reader.

leading edge fit (again based on the rationalization described above) was performed on the aluminum hydride desorption profile, and an activation energy of 0.57 eV was obtained. Winkler report a value of 1.2 eV modeling this system as half-order kinetics.[42] Modeling our data this way gave a value of ~0.69 eV,[52] a value very similar to that obtained for the $m/e = 2$ TPRS data. By themselves, these differences in the energetics do not conclusively demonstrate that the two species followed (H_2 and the aluminum hydride moiety) arise from a true partitioning along separate reaction channels. Such understandings do follow from the beam interaction and the manner in which it effects the desorption kinetics of dihydrogen and aluminum hydride, a matter we consider next.

The data shown in Figures 2 and 3 demonstrate marked impacts derived from the inert gas atom beam. These effects are quantified in Figure 4 which shows the percent reduction in peak area as a function of the flux for each of the three beam energies ($l = 1.6$ eV, $n = 2.8$ eV, and $s = 3.6$ eV). It is evident that, while scaling with the atom flux, the reductions in the peak areas are not linearly dependent. It is particularly noteworthy that the scale of the intensity reduction seen in the two product forming channels are very different; the $m/e = 30$ intensity decreases roughly four times more than does that for $m/e = 2$ for equivalent fluxes. This observation points to a beam interaction that promotes the preferential desorption and/or dissociation of the aluminum hydride species. Since the intensity overall decreases as a result of the beam interaction, we conclude that the collision-induced desorption (CID) of an alane-like species is an efficient and easily promoted process. Since the latter species gives rise to a significant ionization cracking fragment at $m/e = 2$, its loss appears competent to explain the decrease of intensity seen in the $m/e = 2$ channel.

The dynamics of this CID, in principle, are amenable to detailed analysis via their apparent energy scaling and cross-section. The surface area on which an atomic impact yields a desorption event per adsorbed molecule (either H or AlH_3) is the desorption cross-section, Q_D. Ceyer et al. described this relationship thoroughly in the context of a now classic study of the methane/Ni(111) system.[44,53,54] Following that work, the cross section for desorption as a function of the collision energy, flux of the beam (oriented normal to the surface), and the surface coverage can be written as

$$\sum_D\{E_i,\theta,t\} = \frac{-d\theta(t)}{\frac{dt}{F_B\theta(t)}} \quad (1)$$

where E_i is the energy of the incident beam, F_B is the total flux in atoms/cm^2, $q(t)$ is the time dependent surface coverage, and t is the time of exposure to the incident beam.

Integrating eq 1 gives

$$\sum_D\{E_i,\theta\} = \frac{\ln\frac{\theta_o}{\theta_t}}{F_B t} \quad (2)$$

Figure 5 records the cross sections for the various beam energies examined as estimated for three limiting fluxes (● = 1.2×10^{16} collisions/cm^2 exposure, ■ = 3.6×10^{16} collisions/cm^2 exposure, and ▲ = 7.2×10^{16} collisions/cm^2 exposure). It is significant that only those values measured at the smallest total xenon flux (1.2×10^{16} collisions/cm^2) show a sensible energy scaling of the CID cross sections for the alane fragment. Using this latter data as a limiting estimate of the initial cross section (rather than incorporating a further uncertainty by extrapolating the data for each energy to zero flux), we deduce a limiting estimate of the CID threshold energy of ~1 eV. Below this energy, the beam cannot induce a desorption event. For a normal CID process, increasing the beam energy should generally increase the cross section of desorption. This expectation seems to break down very markedly when the cross sections are estimated at larger values of the total integrated flux of the Xe. Clearly, at these longer times, more H atoms have been removed from the surface. The efficiency of this removal, however, *is strongly dependent on both the coverage and bonding states* of the species left behind. In fact, at the longest times, the data suggest that the CID cross section tends towards zero. This somewhat nonphysical result correlates most directly with the depletion of the alane-forming state.

There is one note of caution that we should add here. The kinematic model on which the calculation of a removal cross section is based implicitly assumes that the impacts involve a structurally homogeneous population of species. In point of fact, though, recent elegant STM studies of Reutt-Robey and her co-workers clearly demonstrate that the H atom exposure leads to a massive restructuring of the Al crystal's surface.[55] Their STM data show that the exposure leads to the formation of highly

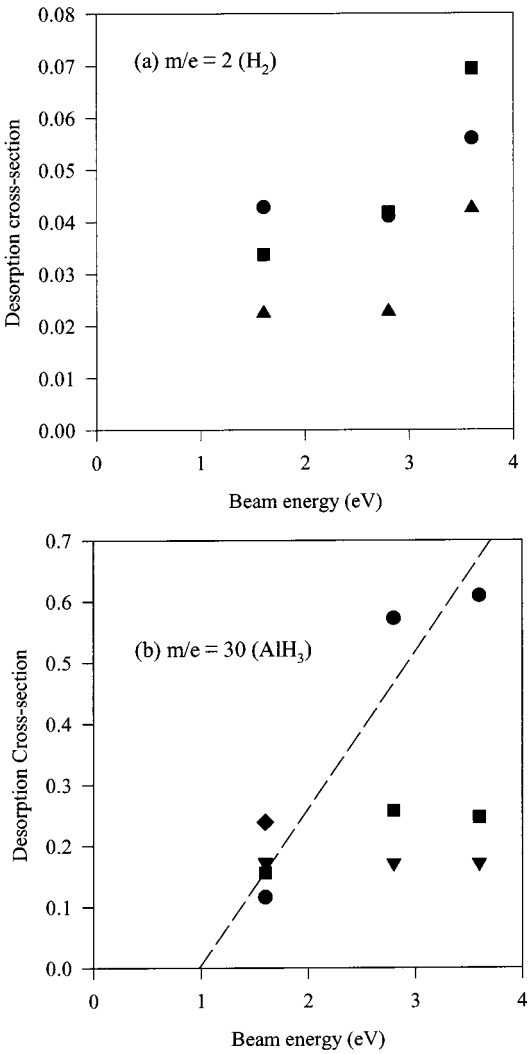

Figure 5. The desorption cross section S_D (Å^2) as a function of beam energy at several fluxes for (a) $m/e = 2$ (H_2^+) and (b) $m/e = 30$ (AlH_3^+). The exposure times are (● = 1.2×10^{16} collisions/cm^2 exposure, ■ = 3.6×10^{16} collisions/cm^2 exposure, ▲ = 7.2×10^{16} collisions/cm^2 exposure). The dashed line in (b) is a linear regression through the 1.2×10^{16} collisions/cm^2 data points used to find the threshold energy level for desorption.

corrugated step edges and significant densities of vacancy island defects. Pinned line defects and step-bunching are also evident in the micrographs. Most striking, though, the authors note that the exposure leads to the formation of a significant density of hydride precipitates that they assign to an alane cluster complex structure. For this reason, the calculated CID threshold energy must be a gross approximation given the apparent heterogeneity of this surface. Beyond this, though, we believe the beam interactions also must alter the states in which the remaining hydrogen atoms are bound; the irreversible changes seen in the TPRS line shapes argue this point very persuasively. This suggests, then, that there must be a state for the adsorbed hydrogen other than that which is readily populated by the exposure to the initial H atom beam under the conditions used to collect the data shown in Figures 1−3. The possible existence of such states is clearly suggested when one notes the sensitivity of the system to dosing effects (as evidenced in the supplemental materials, see below).

The key point to consider with respect to the hyperthermal beam induced effects noted above is that the hydrogen that remains on the surface does not regain its initial configuration upon heating. That is, after exposure to the Xe beam, the system clearly exhibits a change in the desorption kinetics for the hydrogen that remains. This change is both stable (it does not revert back readily to the type of state it populated initially) and shows, in the post-beam TPRS line shapes, desorption kinetics for H_2 that are "mass-action sensitive" to the remaining coverage. The latter point strongly suggests a transition state in which at least one of the H atom partners is mobile. The barrier to the surface diffusion of H on Al is unknown but is expected to be small. The Al−H bond strength is only about 2 eV; the literature suggests a value 10% of this (or ∼0.2 eV) as being a good estimate of the barrier to lateral diffusion. The barrier to diffusion of an isolated H atom in the bulk is known, being only of the order of 0.4 eV. At the temperatures examined here, therefore, one expects an isolated atom to experience nearly free diffusion on the surface. This, then, creates an enormous paradox. Why do we see so many distinct desorption profiles for H_2? It is instructive in this regard to consider the effects that derive from the hyperthermal Xe atom beam. If the hydrogen initially bound were present only on the surface and Xe atoms disrupted this state, why then would a mobile hydrogen atom not repopulate it through simple diffusion? Clearly, there must be some energetic barrier between the before and after-beam states in which the hydrogen is bound—one that cannot be overcome by simple surface diffusion. One can envision several possibilities for the mechanism(s) through which the beam derived collisions lead to gross changes in the TPR spectra of the H remaining on the Al crystal. First, given a model in which the H adsorbed on the surface clusters to form 2D islands, the beam interactions could disrupt these islands. If so, it is hard to envision a reason (given the facile diffusion of H) why the islands would not reform (and in so doing, generate the zero-order rate profiles and product partitioning seen initially). An alternative possibility is that the beam interactions could, via momentum transfer during the collision, implant some of the hydrogen in subsurface sites. The data are less clear as to the viability of this latter mechanism but at least one inferential line of reasoning tends to weigh against it. If this model is correct, then the cross section for the implantation would have to be very large, perhaps almost nonphysically so. The energy scaling noted above does not fit the quantitative estimate of this barrier either (see below), although the differences (∼0.3 eV) may be within the errors of measurement. Clearly, the energetics of H atoms binding at both surface and subsurface sites would have to be such so as to preclude repopulation of surface sites via an efficient thermal equilibration. Information available in the literature does tend to support, in part, the viability of this latter point, as we will discuss below.

The third possibility we can consider follows directly from this latter line of reasoning and is based on a more complex model of the structure of the adsorbate layer generated by the H atom source. As noted above, the complexity of the hydrogen desorption kinetics (and the competitive etching which vies with it) strongly suggests that the H atoms cluster. The structural character of these clusters, whether as islands or hydride precipitates, has not been established independently by diffraction studies. The microscopy studies described above do provide evidence supporting some role for the latter species. In the context of the thermodynamics of the Al−H system, and the high energy of the incident atom used to generate the overlayer, it is appropriate to consider whether the process can lead directly to the population of subsurface binding sites. If so, is it possible that exposure to the xenon beam provides enough energy to promote the hydrogen to surface binding sites (and also desorb

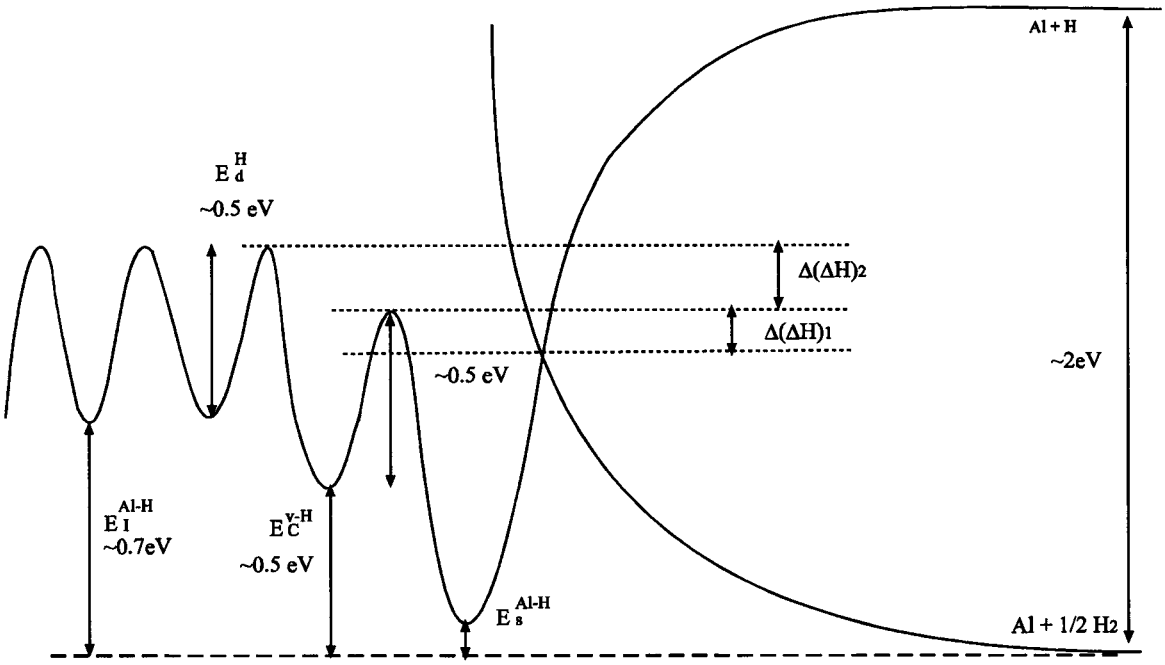

Figure 6. Schematic depiction of the energy profile of hydrogen on/in aluminum.

AlH_3 fragments), and would this help explain the changes seen in the kinetics and product partitioning?

Ceyer et al. performed studies much like the ones undertaken here using a Ni(111) substrate.[56] In that system, molecular hydrogen dissociatively adsorbs on the Ni(111) surface but no further adsorption (or absorption) occurs after the 3-fold hollow sites are filled. The hydrogen, in this case, does not have sufficient energy to dissociatively absorb to a significant degree. After exposure to xenon bombardment with energies >2.6 eV, however, some of the surface hydrogen is absorbed into the bulk. The energy barrier for this transition is ~1 eV. Thus, it is evident that a high energy atom beam can induce changes in the state of adsorbates (and hydrogen in particular) on a single crystal surface and can introduce hydrogen to subsurface binding sites.

Copper, like aluminum, has a large activation energy for the dissociative adsorption of molecular hydrogen. Researchers who study this system also utilize a hot tungsten filament to generate atomic hydrogen to overcome the barrier to the adsorption of the molecular form.[37] Depositing atomic hydrogen on the Cu-(110) surface, for example, does in fact first populate the surface sites. Sandl et al. demonstrated, however, that the energetic hydrogen atoms generated by exposure to a hot tungsten filament (with energies in excess of 2.25 eV) adsorb on the surface and also absorb into subsurface sites.[37] The hydrogen in these subsurface sites desorbs at a temperature approximately 150 K below that for the surface hydrogen because this binding site is ~0.3 eV less favorable. Similarly, the initial energy of the atomic hydrogen should be sufficient to penetrate the surface of nickel (leading to an absorbed state)[57] and Ceyer et al. have backed this hypothesis conclusively with HREELS data.[57,58] In the nickel case, as with copper, it is the surface that saturates first (as it is the lower energy state). One item of concern for studies using a hot filament to dissociate the hydrogen comes from the effects that might result from electron-surface interactions. In a recent paper, Winkler and his co-workers used a hot tungsten nozzle to predissociate the H_2.[59] The TPRS line shapes obtained from Al surfaces dosed in this way closely match those seen in the data shown in Figure 1. This suggests that the hydrogen, as dosed here, occupies states that are directed by the dynamics and energetics of the Al+H interaction rather than radiation effects.

These data, when viewed in conjunction with the latter precedents, strongly suggest that the energy that results from the process used to dissociate the hydrogen in conjunction with the significant exothermicity of the binding should also be enough to embed it into the aluminum. It is to a consideration of this issue that we now turn our attention.

The properties of hydrogen absorbed in bulk aluminum have been studied in great depth.[60,61] There are several lines of evidence derived from this data (beyond the precedents noted above) which point at subsurface hydrogen occupation as a probable configuration for at least some of the hydrogen deposited by the atom beam and the unusual kinetic behavior we see in TPRS.

Buckley and Birnbaum noted that, unlike the majority of fcc metals which undergo lattice expansions of as much as ~2.3 Å per H atom equivalent,[62] aluminum actually undergoes a small contraction of the bulk lattice constant.[58] This unusual behavior results from the formation of bound hydrogen-vacancy complexes.

The energy cost of creating a vacancy in Al is $E_f^v = 0.7$ eV.[61] The energy cost of generating a hydrogen-vacancy complex (C_{v-H}) is even more modest, with $E_f^{v-H} = 0.5$ eV.[61] The surface (being essentially a plane of vacancies) provides a virtually ideal sink for the Al atom displaced to form the C_{v-H} moiety. It is also expected that the barriers associated with promoting this atom to the surface should be small (being essentially a reconstruction to generate the C_{v-H} species) and thus it seems likely that the H atom beam exposure should generate a substantial population of hydrogen bound at both surface and next-layer sites. The near-surface C_{v-H} moieties would, in this sense, represent a softening of the potential surface for Al−H binding. The quantitative aspects of these energy arguments are sketched schematically in Figure 6. As shown in the figure, the absorption of hydrogen into the bulk, where the binding would occur at interstitial sites, would incur an energy cost of ~0.7 eV.[45] Binding in a second layer (or near-surface) site via the formation of a v-H complex would soften

this potential and only require an energy of $E_C^{v-H} \cong 0.5$ eV.[61] As is shown in the figure, the barrier to hydrogen motion in the bulk is also known and, in relative terms, is weakly activated. The literature suggests a value for the barrier to diffusion involving hydrogen bound at interstitial sites is only of the order of ~0.5 eV. The figure also embeds a rather significant assumption about the relative ranking of the various barrier energies. It is instructive to consider this point in the context of the two energy differences denoted as $\Delta(\Delta H)_2$ and $\Delta(\Delta H)_2$. The later barrier height difference $\Delta(\Delta H)_2$ is ranked such that any hydrogen bound in a near surface site must move with a strong asymmetry towards the surface. The understanding of the barrier height$\Delta(\Delta H)_1$ is less certain. The figure is constructed to show this difference as being such that any hydrogen bound in a C_{v-H} form in the second layer would, upon promotion to a surface bound form (presumably with the concomitant annihilation of the vacancy) would recombine and be lost efficiently as H_2 (rather than revert to the initial v−H complex). This latter assumption would suggest that some of the literature estimates of the dissociation barrier to H_2 on Al are, in fact, biased to the high side. This same assumption, as we will develop in detail below, does appear to most completely rationalize all the data reported in this and previous studies of the Al+H system. Before doing so, we turn to a final consideration of the energies that would also warrant consideration in the event that C_{v-H} moieties are formed by the H atom beam.

We ask, how do vacancies interact in bulk? What is more energetically favorable, a set of isolated vacancies or segregated ones (e.g., a divacancy)? It is actually well known that vacancy-vacancy interactions are stabilizing[63,64] and that this effect carries over very strongly (albeit, it is probably softened in relative terms) in C_{v-H} interactions. Indeed, the latter effects underlie the significant tendency of C_{v-H} moieties to nucleate H_2 blisters,[62,65] the latter being an issue of significant interest in the embrittlement of metals[20−22,66] (most interestingly both Ni[67,68]and Al[69] have been studied in some detail in this regard). These precedents strongly suggest that second layer C_{v-H} moieties *should* cluster and thus might provide the structural basis for the correlations evidenced by the zero-order rate profiles seen in TPRS experiments. This clustering would serve to further soften the C_{v-H} binding energy to something less than the 0.5 eV value shown in Figure 6.

The energy diagram shown in Figure 6 embodies one further simplification that warrants comment in light of relevant information available in the literature. There have been studies made by very high resolution scanning transmission electron microscopy (STEM) of hydrogen absorption in thin metal (and alloy) sections. A study of Ni was most instructive in the sense that strong segregation of internal hydrogen toward the crystal surface was seen in this study.[67] The H concentration profile, while peaked at the surface, did not decay to a limiting bulk value at the second metal layer, however. It was found, rather, that the decay ranged over many multiples of the lattice spacing (>5nm). These results suggest that, in addition to facile nucleation of C_{v-H} complexes near the surface, surprisingly long-ranged relaxation effects could soften the bulk E_I^{Al-H} interaction energy for some distance from the surface. Recent theoretical calculations of Al−H absorption processes tend to mirror some aspects of this latter experimentally directed association.[32]

It is interesting to note that with increasing hydrogen coverage, the clarity of the Al(111)(1×1) LEED pattern degrades markedly. Since hydrogen is not visible by LEED, this result cannot be explained by the formation of islands on the surface (a model argued by other researchers), but rather, must involve some sort of relaxation or displacement of the metal atoms. We feel that hydrogen-vacancy complex formation at subsurface sites would offer an explanation for the deterioration of the LEED patterns seen experimentally by us and others.[24,70]

Given the assumption that the H atom exposure generates both a near-surface population of C_{v-H} species as well as surface bound hydrogen, we now consider how the hyperthermal scattering interactions would influence these various bound states. The data presented in Figures 2 and 3 clearly demonstrate that energy transfer at all the collision energies studied decreases the quantity of hydrogen present. It is also strongly demonstrated that this effect is correlated with the depletion of the alane forming state(s). We believe the data most clearly suggest that alane (or a related oligomer) is lost via a collision-induced desorption (CID) process. The beam interactions clearly alter the detailed balance of the structural states of the hydrogen present (as seen in the TPRS data) as well. These latter changes make a calculation of CID cross sections (and thus the threshold energy) very problematic based on the TPRS metric used here. As noted above, these problems are much less pronounced in the data points obtained for the alane fragment for the lowest incident flux of Xe (1.2×10^{16} collisions/cm^2). We can fit the latter data well within the assumptions of the model described above and calculate a threshold energy for the CID of alane (Figure 5). The value estimated in this way, ~1 eV, correlates reasonably with the limiting energies estimated from TPRS. That the dihydrogen cross sections cannot be used to identify a physically plausible activation energy for hydrogen desorption further suggests that the beam activates only one desorption pathway—that which leads to the desorption of alane. We also should note at this point that it seems highly unlikely that this CID process could be generating a third-order recombination of H on a surface Al atom. The cross section for such a process would have to be exceedingly low. This seems to suggest, strongly in our view, that significant hydrogen clustering (perhaps involving C_{v-H} moieties) must be present.

It is most intriguing to note that the alane state can be depleted completely and that the significant quantities of hydrogen left on (or near) the surface do not equilibrate to reform the state which lead to it. This latter aspect of the data is not completely understood but an examination of the energy diagram in Figure 6 does provide some suggestive inferences. Two aspects called out in this figure are of concern here. The first is the absolute magnitude of the C_{v-H} and Al_s−H binding energies and the second is the relative barrier height differences defined by the value $D(DH)_1$. Unfortunately for the context of this discussion, the literature does not provide information that would be needed to rank these values precisely. If the energy transfer from the Xe collisions depletes surface H but leaves behind C_{v-H} species, the changes seen in (and the character of) the TPRS data would then appear to be most consistent with $D(DH)_1$ being positive and the Al_s−H binding energy being somewhat less than that shown in the figure. In this limiting case, then, the kinetics of the H atom motion to the surface would be rate limiting (to a following bimolecular recombination). A variety of rate laws might describe this process with the simplest being a unimolecular dependence on the hydrogen content. A number of other possibilities involving the various rankings of these energies could also lead to rates limited by the hydrogen recombination velocity (which in turn would suggest a second-order dependence of the kinetics on the formal H coverage). For example,

using the above noted depletion argument the motion of the H to the surface could be facile and lead to a rate limited by the recombination step. It is essential to note here that we have no precise understanding of the structural nature of the surface and species left behind by the beam impacts. It is equally plausible, for example, to presume that the etching reaction channel results directly from the presence of C_{v-H} (or surface alane) clusters and that the CID process selectively depletes these states. In this case, one still expects desorption kinetics for H_2 that, in their simplest form, should follow a second-order rate law in the hydrogen coverage.

We attempted to fit the lineshapes shown in Figure 2 (especially for the latter two data sets in which the alane state is largely depleted) to a Redhead model of second-order desorption using a scaled value of the remaining hydrogen to account for its changing CID induced coverage.[71] The results were poor and we thus conclude that a second-order rate law in its simplest form is not a good model of the system. The data is better fit to a first-order rate law and, based on the peak maxima seen, this suggests an activation energy of ~0.9 eV assuming a preexponential factor of 1×10^{13} s^{-1}.[71] This value is, again, well within the uncertainty embedded in the energy diagram shown in Figure 6.

In closing, we remark about the formation of aluminum hydride and related compound phases. Enthalpically, the formation of a bulk aluminum hydride is favorable (−0.04 eV/H atom). It is entropy, however, that makes aluminum hydride unstable at room temperature in a hydrogen-free atmosphere.[61] The entropic factors acting here, however, are certainly affected when the aluminum hydride is present only on the surface or in a subsurface site and thus, the compound may readily form in these regimes. In whatever their form, and as seen in the data shown in Figures 4 and 5, the beam impact preferentially causes the desorption of the material comprising these bound states. Taken together, we believe the data present a very strong argument in support of the hypothesis that the states populated by the atom beam source must involve subsurface occupancies. The hyperthermal collisions of the Xe atoms, via a complex energy exchange process, lead to an irreversible decomposition of these (possibly metastable) initial hydrogen binding states. The details of the dynamics of this energy exchange, one that appears to lead to a collision-iduced desorption of alane-like etching products, remain incompletely understood and warrant further detailed study.

Acknowledgment. We thank the National Science Foundation (CHE 9626871) and the Department of Energy through the Seitz Materials Research Laboratory (DEFG02-96ER45439) for support of this work. We are also deeply appreciative of the many helpful comments given by our colleague, Howard Birnbaum.

Supporting Information Available: Auger electron spectra of an aluminum surface recorded before and after a complete experiment. TPR spectra illustrating the sensitivity of the system to the nature of the electrical bias present during the hydrogen atom exposure. This material is available free of charge via the Internet at http://pubs.acs.org.

References and Notes

(1) Tsubouchi, K.; Masu, K. *Vacuum* **1994**, *46*, 1249.
(2) Littau, A.; Mosely, R.; Zhou, S.; Zhang, H.; Guo, T. *Microelectron. Eng.* **1997**, *33*, 101.
(3) Dubois, L. H.; Zegarski, B. R.; Kao, C. −T.; Nuzzo, R. G. *Surf. Sci.* **1990**, *236*, 77.
(4) Kern, R. *Surf. Sci.* **1980**, *93*, L101.
(5) Kim, C. S.; Bermudez, V. M.; Russel, J. N., Jr. *Surf. Sci.* **1997**, *389*, 162.
(6) Kondoh, E.; Kawano, Y.; Takeyasu, N.; Ohta, T. *J. Electr. Chem. Soc.* **1994**, *141*, 3494.
(7) Kondoh, E.; Ohta, T. *J. Vac. Sci. Technol. A.* **1995**, *13*, 2863.
(8) Sugai, K.; Okabayashi, H.; Shinzawa, T.; Kishida, S.; Kobayashi, A.; Yako, T.; Kadokura, H. *J. Vac. Sci. Technol. B* **1995**, *13*, 2115.
(9) Simmonds, M. G.; Gladfelter, W. L. In *Chemical Aspects of Chemical Vapor Deposition for Metallization*; Kodas, T. T., Hampden-Smith, M. J., Eds.; VCH: New York, 1994.
(10) Spencer, J. T. *Prog. Inorg. Chem.* **1994**, *41*, 145.
(11) Herman, I. P. *Chem. Rev.* **1989**, *89*, 1323.
(12) Dowben, P. A.; Spencer, J. T.; Stauf, G. T. *Mat. Sci. Eng. B* **1989**, *B2*, 297.
(13) Larciprete, R. *Appl. Surf. Sci.* **1990**, *46*, 19.
(14) Aylett, M. R. *Chemtronics* **1988**, *1*, 146.
(15) Shih, D. Y.; Ficolora, P. J. *J. Vac. Sci. Technol. A* **1984**, *2*, 225.
(16) Bent, B. E.; Nuzzo, R. G.; Zegarski, B. R.; Dubois, L. H. *J. Am. Chem. Soc.* **1991**,*113* 1137.
(17) Kao, C. −T.; Dubois, L. H.; Nuzzo, R. G. *J. Vac. Sci. Technol. A* **1991**, *9*, 228.
(18) Bent, B. E.; Nuzzo, R. G.; Dubois, L. H. *J. Am. Chem. Soc.* **1989**, *111*, 1634.
(19) Losser, V.; Küppers, J. *Surf. Sci.* **1993**, *284*, 175.
(20) Besenbacher, F.; Myers, S. M.; Nørskov, J. K. *Nucl. Instrum. Methods Phys. Res., Sect. B* **1985**, *7/8*, 55.
(21) Lufrano, J.; Sofronis, P.; Birnbaum, H. K. *J. Mech. Phys. Solids* **1988**, *46*, 1497.
(22) Sofronis, P.; Birnbaum, H. K. *J. Mech. Phys. Solids* **1995**, *43*, 49.
(23) Myers, S. M. et al. *Rev. Mod. Phys.* **1992**, *64*, 559.
(24) Kondoh, H.; Hara, M.; Domen, K.; Nozoye, H. *Surf. Sci.* **1993**, *287*, 74.
(25) Kondoh, H.; Nishihara, C.; Nozoye, H.; Hara, M.; Domen, K. *Chem. Phys. Lett.* **1991**, *187*, 466.
(26) Hara, M.; Domen, K.; Onishi, T.; Nozoye, H.; Nishihara, C.; Kaise, Y.; Shindo, H. *Surf. Sci.* **1991**, *242*, 459.
(27) Winkler, A.; Pozgainer, G.; Rendulic, K. D. *Surf. Sci.* **1991**, *231*, 886.
(28) Paul, J. *Phys. Rev. B* **1988**, *37*, 6164.
(29) Mundenar, J. M.; Murphy, R.; Tsuei, K. D.; Plummer, E. W. *Chem. Phys. Lett.* **1988**, *143*, 593.
(30) Hara, M.; Domen, K.; Onishi, T.; Nozoye, H. *J. Phys. Chem.* **1991**, *95*, 6.
(31) Gunnarsson, O.; Hjelmberg. H.; Lundqvist, B. I. *Phys. Rev. Lett.* **1976**, *37*, 292.
(32) Hayashi, S.; Hashimoto, E.; Kino, T. *Surf. Sci.* **1994**, *304*, 237.
(33) Jackman, T. E.; Griffiths, K.; Unertl, W. N.; Davies, J. A.; Gurtler, K. H.; Harrington, D. A.; Norton, P. R. *Surf. Sci.* **1987**, *179*, 297.
(34) Rettner, C. T.; Michelson, H. A.; Auerbach, D. J. *J. Chem. Phys.* **1995**, *102*, 4625.
(35) Murphy, M. J.; Hodgson, A. *J. Chem. Phys.* **1998**, *108*, 4199.
(36) Flowers, M. C.; Jonathan, N. B. H.; Morris, A.; Wright, S. *J. Chem. Phys.* **1998**, *108*, 3342.
(37) Sandl, P.; Bischler, U.; Bertel, E. *Surf. Sci.* **1993**, *291*, 29.
(38) Chorkendorff, I.; Rasmussen, P. B. *Surf. Sci.* **1991**, *248*, 35.
(39) Netzer, F. P.; Kneiringer, G. *Surf. Sci.* **1975**, *51*, 526.
(40) Engstrom, J. R.; Tsai, W.; Weinberger, W. H. *J. Chem. Phys.* **1987**, *87*, 3104.
(41) Kim, C. S.; Bermudez, V. M.; Russell, Jr., J. N. *Surf. Sci.* **1997**, *389*, 162.
(42) Winkler, A.; Resch, C.; Rendulic, K. D. *J. Phys. Chem.* **1991**, *95*, 7682.
(43) Lohokare, S. P.; Crane, E. L.; Dubois, L. H.; Nuzzo, R. G. *Langmuir* **1998,** *14*, 1328.
(44) Lohokare, S. P.; Crane, E. L.; Dubois, L. H.; Nuzzo, R. G. *J. Chem. Phys.* **1998**, *108*, 8640.
(45) Boh, J.; Eilmsteiner, G.; Rendulic, K. D.; Winkler, A. *Surf. Sci.* **1998**, *395*, 98.
(46) Harris; Anderson, S. *Phys. Rev. Lett.* **1985**, *55*, 1583.
(47) Duš, R.; Nowicka, E. *Prog. Surf. Sci.* **1998**, *59*, 289.
(48) Christmann, K. *Surf. Sci. Rep.* **1988**, *9*, 1.
(49) He, J. −W.; Harrington, D. A.; Griffiths, K.; Norton, P. R. *Surf. Sci.* **1988**, *198*, 413.
(50) Anger, G.; Winkler, A.; Redulic, K. D. *Surf. Sci.* **1989**, *220*, 1.
(51) King, D. A. *Surf. Sci.* **1975**, *47*, 384.
(52) Parker, D. H.; Jones, M. E.; Koel, B. E. *Surf. Sci.* **1990**, *233*, 65.
(53) Beckerle, J. D.; Johnson, A. D.; Ceyer, S. T. *J. Chem. Phys.* **1990**, *93*, 4047.
(54) Beckerle, J. D.; Johnson, A. D.; Ceyer, S. T. *Phys. Rev. Lett.* **1989**, *62*, 685.
(55) Go, E. P.; Thuermer, K.; Reutt-Robey, J. E. *Surf. Sci.* **1999**, *437*, 377.

(56) Hang, K. L.; Bürgi, T.; Trautman, T. R.; Ceyer, S. T. *J. Am. Chem. Soc.* **1998**, *120*, 8885.
(57) Johnson, A. D.; Maynard, K. J.; Daley, S. P.; Yang, Q. Y.; Ceyer, S. T. *Phys. Rev. Lett.* **1991**, *67*, 927.
(58) Maynard, K. J.; Johnson, A. D.; Daley, S. P.; Ceyer, S. T. *Faraday Discuss. Chem. Soc.* **1991**, *91*, 437.
(59) Pölzl, H.; Strohmeier, G.; Winkler, A. *J. Chem. Phys.* **1999**, *110*, 1154.
(60) Bugeat, J. P.; Chami, A. C.; Ligeon, E. *Phys. Lett.* **1976**, *58A*, 127.
(61) Myers, S. M.; Besenbacher, F.; Nørskov, J. K. *J. Appl. Phys.* **1985**, *58*, 1841.
(62) Buckley, C. E.; Birnbaum, H. K.; Bellmann, D.; Staron, P. *J. Alloys Compds.* **1999**, *295*, 231.
(63) Ades, H. F.; Companion, A. L. *Surf. Sci.* **1986**, *177*, 553.
(64) Young, G. A.; Scully, J. R. *Acta Mater.* **1998**, *46*, 6337.
(65) Clausing, R. E.; Emerson, L. C.; Heaterly, L. *J. Nucl. Mater.* **1978**, *76/77*, 99.
(66) Birnbaum, H. K. In *Encyclopedia of Materials Science and Engineering*; Bever, M. B., Ed.; MIT Press: Cambridge, MA,1984.
(67) Fukushima, H.; Birnbaum, H. K. *Acta Mater.* **1984**, *32*, 851.
(68) Birnbaum, H. K.; Buckley, C.; Zeides, F.; Sirois, E.; Rozenak, P.; Spooner, S.; Lin, J. S. *J. Alloys Compds.* **1997**, *253*, 260.
(69) Ambat, R.; Dwarakadasa, E. S. *Bull. Mater. Sci.* **1996**, *19*, 103.
(70) Nuzzo, R. G.; Bent, B. E.; Dubois, L. H. Unpublished results.
(71) Redhead, P. A. *Vacuum* **1962**, *12*, 203.